

Effective (Floquet) Lindblad generators from spectral unwinding

Görkem D. Dinc, André Eckardt, and Alexander Schnell*

Technische Universität Berlin, Institut für Theoretische Physik, 10623 Berlin, Germany

(Dated: July 8, 2025)

A mathematical description of the reduced dynamics of an open quantum system can often be given in terms of a completely positive and trace preserving (CPTP) map, also known as quantum channel. In a seminal work by Wolf et al. [*Phys. Rev. Lett.* **101**, 150402 (2008)], it was shown that deciding whether a given quantum channel was generated from an underlying effective Markovian dynamics, with time-independent generator of Lindblad form, is generally an NP-hard problem. The difficulty is related to the fact that one has to search through all possible branches of the operator logarithm of the map, in order to identify, if any of the resulting effective generators is of Lindblad form. In this work we show that in cases where one has access to the full reduced dynamics at all previous times (the dynamical map) one can significantly facilitate the search for an effective generator by making use of Floquet theory. By performing a spectral unwinding such that the effective micromotion is minimized, the effective Floquet generator is often an excellent candidate for an effective generator of Lindblad form. This significantly reduces the complexity of the search for an effective Lindbladian in many (though not all) cases. Our results are relevant for engineering Floquet Lindbladians in complex many-body systems.

I. INTRODUCTION

Digital and analog simulation of quantum many-body systems in engineered quantum systems based on photons or atoms have yielded fascinating results [1–18]. Both rely in part on the advent of Floquet engineering [5, 6, 19–21] (which in the context of digital simulation is usually referred to as trotterization [22–29]). The central idea is that for an isolated quantum system with time-periodic Hamiltonian $H(t) = H(t + T)$, the one-cycle time-evolution operator $U(T)$ can be rewritten as $U(T) = \exp(-iH_F T)$ with a time-*independent* Floquet Hamiltonian H_F with possibly novel terms that are not present in the lab Hamiltonian, e.g. artificial gauge fields [3–6, 19, 30–33] or nontrivial interactions [13, 34–39].

Recently, the question was raised [40–42] whether these ideas can be generalized to *open* Floquet systems [43], i.e. systems that interact with an environment (e.g. by coupling the system to external photon or particle reservoirs). Interestingly, it was shown [41] that the dynamics under a time-periodic Lindbladian $\mathcal{L}(t) = \mathcal{L}(t + T)$ [27, 41, 44–47] cannot always be understood as generated from an effective time-independent Floquet Lindbladian \mathcal{L}_F [40–42, 44, 48–52]. This is due to effective non-Markovian effects that are built up during the evolution. As a result of the existence of branches when calculating the complex logarithm of the dynamical map, deciding whether a valid Floquet Lindbladian exists is generally an NP-hard problem [53]. This question closely relates to earlier work by Wolf et al. [53, 54] where the existence of an effective Lindbladian generator was studied for a snapshot in time of a general quantum evolution \mathcal{V} , a completely positive and trace-preserving (CPTP) map, irrespective of where it originates from. In this work, we show that by using ideas from Floquet theory, the general

problem of deciding Markovianity can be addressed more efficiently in cases where one does not only have access to such a snapshot in time, but also to the full dynamical map $\mathcal{V}(t)$ for all times t . This is relevant, e.g. for Floquet engineering of open quantum systems, where such effective Lindbladian generators can capture the system’s stroboscopic dynamics and hence be utilized in the same manner as Floquet Hamiltonians in the case of isolated systems. Our results lay the foundation for Floquet engineering of Lindbladians in extended many-body systems.

II. MARKOVIANITY TEST

The mathematical cornerstone of the theory of Markovian open quantum systems are one-parameter semigroups $\mathcal{V}(t)$ which are superoperators on the Hilbert space \mathcal{H} with dimension d . The semigroup $\mathcal{V}(t) = e^{\mathcal{L}t}$, $t \geq 0$, describes an evolution of the density operator $\varrho(t) = \mathcal{V}(t)[\varrho(0)]$ that is Markovian and consistent with a physical evolution, if the *dynamical map* $\mathcal{V}(t)$ is CPTP, i.e. a *quantum channel*, at all times t . Lindblad [55], Gorini, Kossakowski and Sudarshan [56] have shown that a superoperator \mathcal{L} is the generator of a quantum dynamical semigroup $\mathcal{V}(t) = e^{\mathcal{L}t}$, iff it can be expressed as

$$\mathcal{L}[\cdot] = -i[H, \cdot] + \sum_{i,j=1}^{d^2-1} G_{ij} \left(F_i \cdot F_j^\dagger - \frac{1}{2} \{ F_j^\dagger F_i, \cdot \} \right), \quad (1)$$

where we set $\hbar = k_B = 1$, $\{\cdot, \cdot\}$ denotes the anti-commutator, $H = H^\dagger$ the Hamiltonian, G_{ij} a positive semidefinite Kossakowski matrix, and F_i a basis of traceless operators. \mathcal{L} is called a *Lindblad superoperator* or *Lindbladian*.

Let us turn to the converse question and ask “Given an arbitrary quantum channel \mathcal{V} (say at time T) is there an effective generator

$$\mathcal{S} = \log(\mathcal{V})/T \quad (2)$$

* schnell@tu-berlin.de

that has Lindblad form as in Eq. (1)?". Due to the multi-valuedness of the complex logarithm, this question turns out to result in an NP-hard problem in general, also called the *Markovianity problem* [53, 54]. A criterion for Markovianity in this sense was proposed by Wolf et al. [53, 54]: A generator \mathcal{S} has Lindblad form, iff (i) for all Hermitian $\kappa = \kappa^\dagger$, \mathcal{S} preserves Hermiticity, i.e. $\mathcal{S}[\kappa] = (\mathcal{S}[\kappa])^\dagger$, and (ii) \mathcal{S} is *conditionally completely positive* (CCP), i.e.

$$(\mathbf{1}_{d^2} - \Sigma)\mathcal{S}^\Gamma(\mathbf{1}_{d^2} - \Sigma) \geq 0. \quad (3)$$

Here, $\Sigma = |\Omega\rangle\langle\Omega|$ is the projector onto the maximally entangled state $|\Omega\rangle = \frac{1}{\sqrt{d}} \sum_{j=1}^d |j\rangle \otimes |j\rangle$ of the system and an ancilla of same dimension d and

$$\mathcal{S}^\Gamma = d \cdot (\mathcal{S} \otimes \mathbf{1}_d)[\Sigma] \quad (4)$$

denotes the Choi representation of \mathcal{S} . Since the complex logarithm is not uniquely defined, we need to check if there is a branch of the operator logarithm of \mathcal{V} that satisfies condition (i) and (ii).

To do this, we introduce the operator scalar product $(A|B) = \text{Tr}[A^\dagger B]$. By also defining an orthonormal operator basis $\{F_\alpha\}_{\alpha=1}^{d^2}$, we can represent quantum channels \mathcal{V} as matrices $\hat{\mathcal{V}}$, with their corresponding matrix elements $\hat{\mathcal{V}}_{\alpha\beta} = (F_\alpha|\mathcal{V}|F_\beta)$, which allows for the identification $\varrho = |i\rangle\langle j| \rightarrow |\varrho\rangle = |i, j\rangle$, known as vectorization of (density) matrices. A useful operation is $\mathbb{F}[\sum_{i,j} c_{ij}|i, j\rangle] = \sum_{i,j} c_{ij}^*|j, i\rangle$ [54]. Assuming the map $\hat{\mathcal{V}}$ to be non-defective, which is generally justified for Markovian maps and quantum channels [53], we first cast it into Jordan normal form [54],

$$\hat{\mathcal{V}} = \sum_r \lambda_r |r_r\rangle (l_r) + \sum_{c=1}^{N_c} [\lambda_c |r_c\rangle (l_c) + \lambda_c^* \mathbb{F} |r_c\rangle (l_c) \mathbb{F}], \quad (5)$$

with r and c indexing the real and complex eigenvalues, respectively, and N_c the total number of complex conjugated pairs. The logarithm yields a family of possible generators of \mathcal{V} [41, 54],

$$\hat{\mathcal{S}}_{\vec{x}} = \hat{\mathcal{S}}_0 + i \frac{2\pi}{T} \sum_{c=1}^{N_c} x_c \left[|r_c\rangle (l_c) - \mathbb{F} |r_c\rangle (l_c) \mathbb{F} \right], \quad (6)$$

with $\hat{\mathcal{S}}_0$ stemming from the principal branch of the logarithm and a vector $\vec{x} = \{x_1, x_2, \dots, x_{N_c}\} \in \mathbb{Z}^{N_c}$ of integers labeling the possible branches of the complex logarithm. Note that, to arrive at Eq. (6), we implicitly assume that condition (i) is fulfilled [41, 54], i.e. that all real eigenvalues λ_r of $\hat{\mathcal{V}}$ are positive [57]. Naively, to test condition (ii), we have to inspect all branches, i.e., a countably infinite number of combinations of N_c integers. Nevertheless, by use of methods from integer programming, the problem can be reduced to a smaller set of possible integers [53], or alternatively one can apply machine-learning algorithms [58].

However, it was shown [53] that deciding Markovianity is generally an NP-hard problem. This is especially detrimental in the case of interacting many-body systems where already the underlying Hilbert space \mathcal{H} grows exponentially with system size L . Consider for example a spin chain of length L , with $d = \dim(\mathcal{H}) = 2^L$. If we would just naively check the two closest branches around the principle branch, i.e. $x_c \in \{-1, 0, 1\}$, we already find super exponential scaling $3^{2^{2L-1}-1}$ of the number of branches for which condition (ii) has to be checked.

In the case that no branch gives rise to a valid Lindbladian, one can measure the distance to Markovianity and find the branch that is closest to a Markovian evolution. We use a measure proposed by Wolf et al. [54] that is based on adding a noise term $\chi \mathcal{Z}$ of strength χ to the generator $\mathcal{S}_{\{\vec{x}\}}$, where \mathcal{Z} is the generator of the depolarizing channel. The distance from Markovianity is defined as [54]

$$\mu = \min_{\{\vec{x}\} \in \mathbb{Z}^{N_c}} \min \left\{ \chi \geq 0 \mid \mathcal{S}_{\{\vec{x}\}} + \chi \mathcal{Z} \text{ is CCP} \right\}, \quad (7)$$

i.e. the minimal strength needed, such that the generator $\mathcal{S}_{\{\vec{x}\}} + \chi \mathcal{Z}$ is Lindbladian. Details on the definition and how to calculate this measure μ are laid out in Refs. [41, 54].

III. SYSTEMS WITH ACCESS TO FULL TIME-DEPENDENT MAP

We describe a strategy that allows to address (and often solve) this problem in cases, where additionally to \mathcal{V} at time T , the full dynamical map $\mathcal{V}(t)$ is known also for times $t \in [0, T]$. To this end, we draw a connection to Floquet theory by continuing $\mathcal{V}(t)$ periodically for $t > T$, e.g. $\mathcal{V}(t) = \mathcal{V}(t-T)\mathcal{V}(T)$ for $T < t \leq 2T$ and so on (a similar strategy was employed in the context of isolated systems for the purpose of adiabatically preparing eigenstates of time evolution operators [59]). Then, the time evolution can effectively be understood as generated from a time-periodic generator $\mathcal{G}(t) = \mathcal{G}(t+T)$ (not necessarily of Lindblad form) since

$$\partial_t \varrho(t) = [\partial_t \mathcal{V}(t)] \mathcal{V}(t)^{-1} \varrho(t) = \mathcal{G}(t) \varrho(t), \quad (8)$$

where we assume that $\mathcal{V}(t)$ is differentiable and invertible.

Let us briefly discuss Floquet theory for isolated (and open) systems. For systems with time-periodic Hamiltonian $H(t) = H(t+T)$ (generator $\mathcal{G}(t)$), the fundamental solutions can be written in terms of Floquet states $|\psi_\alpha(t)\rangle = \exp(-i\varepsilon_\alpha t) |u_\alpha(t)\rangle$ ($|\varrho_\mu(t)\rangle = \exp(-i\Omega_\mu t) |\Phi_\mu(t)\rangle$) with time-periodic Floquet modes $|u_\alpha(t)\rangle = |u_\alpha(t+T)\rangle$ ($|\Phi_\mu(t)\rangle = |\Phi_\mu(t+T)\rangle$) [20, 42, 60] and quasienergies ε_α [20] (eigenvalues Ω_μ). In case of a purely coherent evolution, $\mathcal{G}(t) = -i[H(t), \cdot]$, the Ω_μ correspond to *quasienergy differences* (a term that we will continue to use also for the dissipative

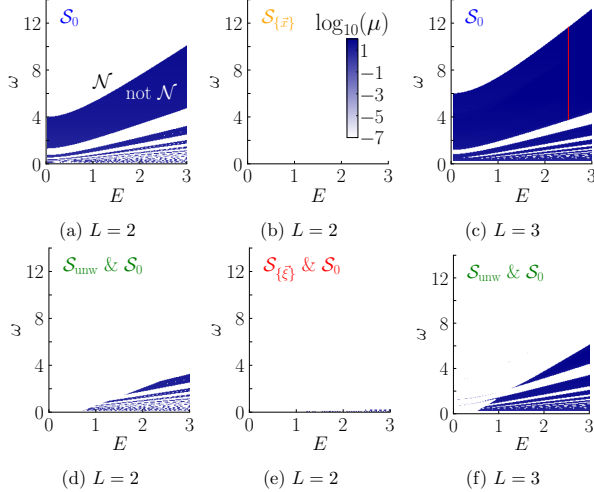


FIG. 1. (a)-(f) Distance from Markovianity μ (which here equals to distance from von Neumann form \mathcal{N}) of the effective generator of the one-cycle evolution superoperator as a function of driving strength E and frequency ω , for no dissipation, $\gamma = 0$, coupling strength $w = 0.1$, and chain lengths of (a),(b),(d),(e) $L = 2$ and (c),(f) $L = 3$. To avoid numerical artifacts stemming from degeneracies in the spectrum of $\mathcal{V}(T)$, we set $\Delta_1 = 1.01, \Delta_2 = 1.00, \Delta_3 = 0.98$.

case). Note that the quasienergies ε_α (quasienergy differences Ω_μ) are not uniquely defined and can be redefined under the gauge transformation $\varepsilon_\alpha \rightarrow \varepsilon_\alpha + m\omega$ and $|u_\alpha(t)\rangle \rightarrow e^{im\omega t}|u_\alpha(t)\rangle$ ($\Omega_\mu \rightarrow \Omega_\mu + m\omega$ and $|\Phi_\mu(t)\rangle \rightarrow e^{im\omega t}|\Phi_\mu(t)\rangle$), where $\omega = 2\pi/T$ and $m \in \mathbb{Z}$. In the isolated case, picking a specific gauge is equivalent to fixing the branch of the complex logarithm when solving for $H_F = i\log[U(T)]/T$. Stroboscopically, at $t = 0, T, 2T, \dots$ the time evolution operator $U(T) = \exp(-iH_F T)$ is described by the effective time-independent Floquet Hamiltonian

$$H_F = \sum_\alpha \varepsilon_\alpha |u_\alpha(0)\rangle\langle u_\alpha(0)|. \quad (9)$$

In the dissipative case, for a given time t , we can decompose the dynamical map $\hat{\mathcal{V}}(T)$ as

$$\hat{\mathcal{V}}(T) = \sum_\mu e^{-i\Omega_\mu T} |\Phi_\mu(T)\rangle\langle \tilde{\Phi}_\mu(0)|, \quad (10)$$

with the left Floquet modes $(\tilde{\Phi}_\mu(t)|$ being different from the right ones for dissipative systems with a non-hermitian generator [42]. In this way, we can immediately identify the effective generator as [42]

$$\hat{S} = - \sum_\mu i\Omega_\mu |\Phi_\mu(0)\rangle\langle \tilde{\Phi}_\mu(0)|, \quad (11)$$

with the freedom of choosing the Floquet gauge of the quasienergy differences Ω_μ indicating the freedom of choosing a branch of the logarithm in Eq. (6).

Let us now, for illustrative purposes, regard the evolution with a time-independent generator, $\partial_t \varrho(t) = \mathcal{L}\varrho(t)$, such that $\mathcal{V}(T) = \exp(\mathcal{L}T)$, as an effective time-periodic problem with arbitrary period T . If we choose a large T such that $\omega = 2\pi/T$ is smaller than the imaginary part of some of the eigenvalues of \mathcal{L} , we observe that the generator \mathcal{S}_0 that we obtain from the principle branch of $\log(\mathcal{V}(T))/T$ is *not* identical to \mathcal{L} but there occurs a “winding” of the eigenvalues of the Floquet generator \mathcal{S} “around” the first *Floquet Brillouin zone*, $\text{Re}[\Omega_\mu] \in [-\omega/2, \omega/2]$, since $\exp(-i\Omega_\mu T)$ has the shape of a circle. This winding turns out to make the previously outlined procedure of searching around the principle branch inefficient, even for a fully coherent time evolution with *no* dissipation: To demonstrate this, we consider a circularly driven spin chain of length L

$$H(t) = \sum_{\ell=1}^L \frac{\Delta_\ell}{2} \sigma_z^\ell + \sum_{\ell=1}^{L-1} w \sigma_x^\ell \sigma_x^{\ell+1} + H_{\text{drive}}(t) \quad (12)$$

$$H_{\text{drive}}(t) = \sum_{\ell=1}^L E [\cos(\omega t) \sigma_x^\ell - \sin(\omega t) \sigma_y^\ell], \quad (13)$$

with level splitting Δ_ℓ , coupling strength w between neighbouring spins, driving strength E and -frequency ω . As we show in Fig. 1(a) and (c), even if we calculate the dynamical map $\mathcal{V}(T)$ for an evolution with time-dependant von-Neumann generator $\mathcal{G}(t) = -i[H(t), \cdot]$, the generator \mathcal{S}_0 of the principle branch is *not* necessarily of von-Neumann form \mathcal{N} (and neither of Lindblad form), see blue areas. This is in stark contrast to our knowledge of the existence of the Floquet Hamiltonian H_F , i.e. $\mathcal{S} = -i[H_F, \cdot]$ is a valid effective Lindblad generator. Only after also searching around the first two neighbouring branches, i.e. $x_c \in \{-1, 0, 1\}$, one finds again a valid von Neumann generator, as we show in Fig. 1(b). However, for every point in the phase diagram, a maximal number of $3^{2^{2L-1}-1}$ branches has to be checked for condition (ii). Due to the super exponential scaling, for $L = 3$ ($L = 4$) we would already have a maximal number of $\approx 6 \cdot 10^{14}$ ($\approx 3 \cdot 10^{60}$) branches to consider, simply to avoid the winding problem (cf. yellow line in Fig. 2(a)). In order to avoid this problem, we propose a different approach which is based on a strategy for unwinding the quasienergy spectrum.

IV. SPECTRAL UNWINDING

For undriven systems it is straightforward to define an “unwinding” procedure that undoes this winding into the first Floquet Brioullin zone: Since the Floquet modes $|\Phi_c(t)\rangle$ with corresponding complex quasienergy differences Ω_c are time-periodic, we can expand them in a Fourier series

$$|\Phi_c(t)\rangle = \sum_{n \in \mathbb{Z}} e^{i\omega n t} |\Phi_c^{(n)}\rangle, \quad (14)$$

and compute the trace norm for all of their Fourier components $\|\Phi_c^{(n)}\| = \text{Tr} \sqrt{\Phi_c^{\dagger(n)} \Phi_c^{(n)}}$. For every mode c we determine

$$x_c^{(\max)} = \arg \max_{x \in \mathbb{Z}} \{\|\Phi_c^{(x)}\|\}. \quad (15)$$

Then, we shift the Ω_c by this number of quanta $x_c^{(\max)}$ giving the ‘unwound’ Floquet generator

$$\hat{\mathcal{S}}_{\text{unw}} = \hat{\mathcal{S}}_0 + i\omega \sum_{c=1}^{N_c} x_c^{(\max)} \left[|\Phi_c(0)(\tilde{\Phi}_c(0)| - |\mathbb{F}|\Phi_c(0)(\tilde{\Phi}_c(0)|\mathbb{F}) \right] \quad (16)$$

In the undriven system, this gauge transformation removes the micromotion and transforms the Floquet modes into the static eigenmodes of the time-independent generator \mathcal{G} [20, 61]. We now show that this procedure also significantly improves the search for an effective generator in the case of a time-dependent generator $\mathcal{G}(t)$. In Fig. 1(d) and (f) we show the phase diagrams we obtain from checking the principle branch \mathcal{S}_0 and the unwound generator \mathcal{S}_{unw} for chain lengths $L = 2$ and $L = 3$. Here, between \mathcal{S}_0 and \mathcal{S}_{unw} , we choose the generator with shortest distance from Markovianity μ . In Appendix A, we plot the phase diagrams of \mathcal{S}_0 and \mathcal{S}_{unw} separately. By using the procedure above, in comparison to Fig. 1(a) and (c), we find that specifically in the high-frequency regime we obtain a lot more points (E, ω) yielding generators of von Neumann form. (In App. B, we introduce a measure to determine the distance from the von-Neumann form and show that both measures almost coincide for our problem.)

However, as we observe in Fig. 1(d),(f) for low frequencies, this method of unwinding fails. This is expected, since in this regime the peaks in the Fourier spectra can become more broadly distributed over several Fourier modes and indistinctly peaked, which we illustrate in App. C, by specifically analyzing the Fourier spectra of $\|\Phi_c^{(n)}\|$ at points, where \mathcal{S}_{unw} fails and succeeds in giving a valid generator of von Neumann form. To overcome this issue, one has to include additional frequency peaks for the search in this regime. In the following, we outline how to find well-chosen candidates for effective generators to test for Markovianity, other than \mathcal{S}_0 and \mathcal{S}_{unw} . To this end, we set $x_c^{(\max,0)} = x_c^{(\max)}$ and choose a number $\eta \in [0, 1]$, which determines at which amplitude ratio we want to include the neighbouring peaks $x_c^{(\max,i>0)}$ into the possible branch combinations. The resulting family of generators $\hat{\mathcal{S}}_{\{\xi\}}$ we consider is given by

$$\{\vec{\xi}\} = \left\{ (\xi_i) \in \mathbb{Z}^{N_c} \mid \xi_c \in \{x_c^{(\max,0)}, \dots, x_c^{(\max,z_c)}\} \right\}, \quad (17)$$

where for every pair of complex modes c , we include the z_c neighbouring Fourier peaks with amplitudes $A_c^{(\max,i)}/A_c^{(\max,0)} \geq \eta$, with $A_c^{(\max,i)} = \|\Phi_c^{(x^{(\max,i)})}\|$. We additionally introduce a cutoff N_b for the maximal

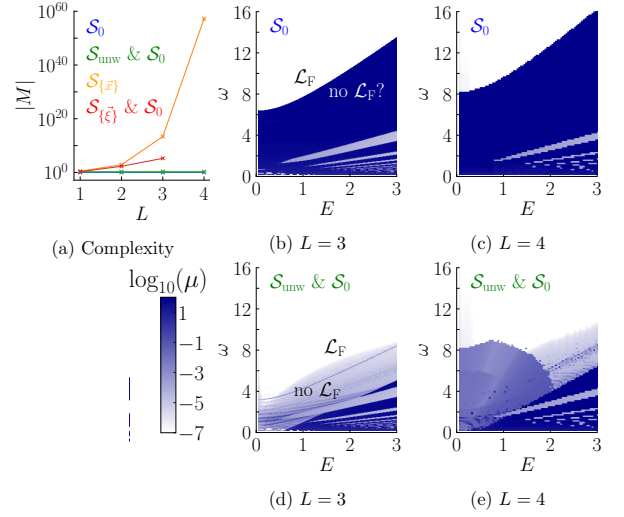


FIG. 2. (a) Cardinality $|M|$ of the set M of possible branch combinations for the different methods and lengths L . (b)-(e) Distance from Markovianity μ of the effective generator of the one-cycle evolution superoperator as a function of driving strength E and frequency ω , for weak dissipation $\gamma = 0.01$, bath temperature $\mathcal{T} = 1$ and chain lengths of (b),(d) $L = 3$ and (c),(e) $L = 4$. Other parameters $\Delta_1 = 1.4$, $\Delta_2 = 1.1$, $\Delta_3 = 0.7$, $\Delta_4 = 0.9$, $w = 0.01$.

number of branches considered, i.e. $z_c \leq N_b$. This gives rise to a systematic search around the unwound generator \mathcal{S}_{unw} , instead of searching around the generator of the principle branch \mathcal{S}_0 , which can drastically reduce the required numerical effort. In Fig. 1(e) we apply this modified Markovianity test for a spin chain of length $L = 2$ and parameters $N_b = 2, \eta = 0.7$. We observe that we almost fully recover valid von Neumann generators. Note that for $L \geq 3$ this choice of N_b and η will not suffice to recover valid von Neumann generators in every point of the phase diagram. Here, to minimise the numerical effort, for a given point, one can search for the smallest N_b and largest η which yield a generator of von Neumann form. In App. D, for $L = 3$ we have set $N_b = 1$ and varied η to find an optimum along the vertical red line at $E = 2.5$ in Fig. 1(e).

To compare the reduction in complexity of our method to the naive procedure of searching around the principle branch, in Fig. 2(a) we plot the cardinality $|M|$ of the set M of all possible branch combinations for which we test for Markovianity. For the principle branch \mathcal{S}_0 we always have $|M| = 1$ (blue line). The generators of the principle branch yield poor results due to the winding of quasienergy differences. Including the first two neighbouring, i.e. $x_c \in \{-1, 0, 1\}$, fixes this problem, but greatly increases the complexity as we see for the orange line. On the other hand, trying to revert the winding by only including \mathcal{S}_0 and \mathcal{S}_{unw} , we have $|M| = 2$ (green line). Using the modified Markovianity test of Eq. (17), the red line in Fig. 2(a) shows the minimal cardinality needed to obtain a fully von Neumann phase diagram for $L = 2$, as

well as to make the points on the red line in Fig. 1(c) fully von Neumann for $L = 3$. For $L = 3$ we have $|M| \approx 10^5$ on average (see App. D for details). Searching around the principle branch requires $|M| \approx 10^{13}$. This shows that searching around the unwound generator dramatically decreases the complexity (as long as we are not at low frequencies, where the peaks in the Fourier spectra may spread across multiple Fourier modes). For systems with large Hilbert space dimensions, where it is numerically impossible to test all branch combinations when considering e.g. the principal and first two neighbouring branches, i.e. $x_c \in \{-1, 0, 1\}$, the conventional method would require to blindly guess a branch combination with no physical or mathematical justification, while our method provides a systematic way of searching for new generators in cases where the principle branch \mathcal{S}_0 and unwound generator \mathcal{S}_{unw} yield poor results. Nevertheless, even for the modified method, the complexity still grows fast with the dimensionality of the problem, which is why for bigger systems one might only be able to include the principle branch \mathcal{S}_0 and the unwound generator \mathcal{S}_{unw} (or alternatively, combine our method with the existing machine learning method of Ref. [58]).

V. DISSIPATIVE CASE

In the case of a coherent time evolution we can always compute a Floquet Hamiltonian H_F and then obtain the effective time-independent Floquet generator $\mathcal{S} = -i[H_F, \cdot]$, which always has von Neumann form. Such a bypass, however, is not possible in the case of dissipative systems where we search for effective time-independent generators of Lindblad form, i.e. Floquet Lindbladians [41, 42]. Here we have to compute $\log(\mathcal{V}(T))/T$ and test these generators for Markovianity [41]. If we do not change the Hamiltonian but add very weak dissipation, we can see exactly the same non-Markovian areas arising in the principle branch, cf. Fig. 2(b). Here, we add dissipation described by Lindblad jump operators for the quantum-optical master equation

$$L_{kq}^\ell = \sqrt{R_{kq}^\ell} |\psi_k\rangle\langle\psi_q|, \quad (18)$$

where, for simplicity, we neglect the impact of the driving term on the dissipator. Hence, $|\psi_k\rangle, E_k$ are the many-body eigenstates and -energies of the undriven Hamiltonian for $E = 0$, respectively. The corresponding jump rate for contact with a reservoir at temperature \mathcal{T} at site l reads

$$R_{kq}^\ell = 2\pi\gamma^2 |\langle\psi_k|\sigma_x^\ell|\psi_q\rangle|^2 g(E_k - E_q) \quad (19)$$

with $g(E) = E/(e^{E/\mathcal{T}} - 1)$, assuming an ohmic bath [62].

By summing over all jump operators we obtain the

total time-periodic Lindbladian

$$\mathcal{L}(t)[\cdot] = -i[H(t), \cdot] + \sum_{\ell=1}^L \sum_{k,q} (L_{kq}^\ell \cdot L_{kq}^{\ell\dagger} - \frac{1}{2} \{L_{kq}^{\ell\dagger} L_{kq}^\ell, \cdot\}). \quad (20)$$

Only considering the generator of the principle branch \mathcal{S}_0 , for $L = 3$ and $L = 4$, we obtain the maps shown in Fig. 2(b) and (c), respectively. Applying the Markovianity test to the unwound Floquet generator \mathcal{S}_{unw} and \mathcal{S}_0 yields the phase diagrams in Fig. 2(d) and (e), where we observe that the phase diagrams contain more valid Floquet Lindbladians \mathcal{L}_F (white region) [41, 42] or have significantly lower distances from Markovianity μ in the areas where no \mathcal{L}_F exists. Note again that scanning through all the possible logarithm branches would mean to scan through possibly $\approx 10^{14}$ candidates for $L = 3$ and $\approx 10^{60}$ candidates for $L = 4$, if we merely wanted to include the first two neighbouring branches $x_c \in \{-1, 0, 1\}$. The unwound generator \mathcal{S}_{unw} thus gives rise to a fast way of determining a particularly good candidate generator which can be tested for Markovianity, when dealing with high-dimensional open quantum many-body systems. In App. E we provide further observations for interacting systems in terms of the existence of the Floquet Lindbladian. Based on that, we motivate our specific choice of dissipation in this paper. In App. F we further give an example to show that the unwound generator is a good candidate not only for Floquet systems but also in the general case of a time-dependent non-periodic map $\mathcal{V}(t)$. We show that for a convex combination

$$\mathcal{V}(t) = \lambda\mathcal{V}_1(t) + (1 - \lambda)\mathcal{V}_2(t), \quad (21)$$

where $\mathcal{V}_j(t) = e^{t\mathcal{L}_j}$ with Lindbladians \mathcal{L}_j and $\lambda \in [0, 1]$ (which previously has been studied in the context of definitions of Markovianity [63]) the unwound generator \mathcal{S}_{unw} produces valid effective Lindbladians in areas where the generator of principle branch \mathcal{S}_0 does not.

VI. SUMMARY

We have demonstrated that the problem of deciding Markovianity [54] (i.e. deciding whether a given quantum channel was generated by a Lindbladian generator) can often be solved for cases with access to the full dynamical map. To this end, we employ Floquet theory and perform a gauge transformation that minimizes the occurring micromotion. Our ideas also significantly simplify the calculation of effective Floquet-Lindbladians for complex many-body systems [41, 42, 58] and can be applied in the context of Liouvillian learning [27] for trotterized open quantum systems. Remarkably, already without dissipation, we have shown that the effective Floquet generator is generally not of von Neumann form. This highlights the fact that, while for the Hamiltonian case any branch of the quasienergy spectrum yields a sensible description, for Liouvillians one has to be much more

careful, since only some branches provide a valid physical description.

ACKNOWLEDGMENTS

This work was partially supported by the Deutsche Forschungsgemeinschaft (DFG, German Research Foundation) via the Research Unit FOR 5688 (Project No. 521530974). G. D. acknowledges support from a fellowship of the German Academic Exchange Service (DAAD).

Appendix A: Phase diagram with and without dissipation

In Fig. 3 we show how the phase diagrams of \mathcal{S}_0 and \mathcal{S}_{unw} complement each other in the coherent and dissipative case.

Appendix B: Von-Neumann measure

An arbitrary effective generator $\mathcal{S}_{\{\vec{x}\}}$ has von Neumann form if the left hand side of Eq. 3 of the main text vanishes [42]

$$(\mathbf{1}_{d^2} - \Sigma)\mathcal{S}_{\{\vec{x}\}}(\mathbf{1}_{d^2} - \Sigma) \equiv \mathcal{M}_{\{\vec{x}\}} = 0. \quad (\text{B1})$$

Thus, to compute the minimal deviation from von Neumann form, we use the norm $\|\mathcal{M}_{\{\vec{x}\}}\|_1 = \text{Tr} \sqrt{\mathcal{M}_{\{\vec{x}\}}^\dagger \mathcal{M}_{\{\vec{x}\}}}$ and introduce the measure

$$\nu = \min_{\{\vec{x}\} \in \mathbb{Z}^{N_c}} \left\{ \|\mathcal{M}_{\{\vec{x}\}}\|_1 \right\}, \quad (\text{B2})$$

which we interpret as ‘‘distance from von Neumann form’’. In Fig. 4 we can observe that we obtain the same zero-distance area in parameter space as in Fig. 1 in the main text, whereas the precise values of the measures in the area of non-zero measure slightly deviate.

Appendix C: Fourier spectrum analysis for the success of the spectral unwinding procedure

The reason for the failure of the procedure at certain points in the phase diagram can be analyzed by investigating the Fourier spectra of the Floquet modes. An example is plotted in Fig. 5, where in (a) and (b) we show the same phase diagrams as in Fig. 1(c) and (f) of the main text, respectively, and in (c) we analyze the Fourier spectra of $\|\Phi_c^{(n)}\|$ for a specific Floquet mode c , as a function of n . The different curves correspond to the points in (a) and (b). We can see that for $\omega = 3, 6, 10$, where the procedure gives good results for \mathcal{S}_{unw} (compare (a) and (b)), the modes are distinctly peaked. However,

for $\omega = 4$ (orange), the procedure fails for \mathcal{S}_{unw} . Note that here $\|\Phi_c^{(-1)}\|, \|\Phi_c^{(0)}\|, \|\Phi_c^{(+1)}\|$ are peaked similarly such that for this point in phase space, all three n should be considered.

Appendix D: Details on the complexity of the modified Markovianity test for $L = 3$

As mentioned in the main text, for $L \geq 3$ we cannot set N_b and η to any arbitrary values and expect to recover valid von Neumann generators for every single point in the phase diagram while also ensuring that the results can be obtained in reasonable computation times. Thus, for $L \geq 3$, for every point in the phase diagram one can pick an N_b and η and check if one obtains the correct branch combination. If yes (not), one can readjust the parameters by decreasing (increasing) N_b and/or increasing (decreasing) η . As a consequence, this readjustment will decrease (increase) the complexity in terms of the computation time. In Fig. 1(e) of the main text (chain length $L = 3$) we have set $N_b = 1$ and varied η for the vertical red line at $E = 2.5$. The interval $\omega \in [3.8, 11.7]$ that we consider, only contains points where the generator of the principle branch \mathcal{S}_0 does not yield a proper von Neumann generator. Starting at $\omega = 3.8$ and using increments of $\Delta\omega = 0.1$, for every point we have numerically determined the largest value of η which yields a valid generator of von Neumann form. The results are shown in Tab. I. Note that for $\omega \in [5.0, 11.7]$ the unwinded generator \mathcal{S}_{unw} already constitutes the correct branch.

In order to compare the complexity between the methods, we have quantified the complexity using the cardinality $|M|$ of the set M of considered branches for the different methods. For the standard Markovianity test, considering solely $x_c \in \{-1, 0, 1\}$ (since this choice is enough to recover valid von Neumann generators everywhere), the size of M is determined by the number of neighboring branches to the principal branch that are included and the number of complex conjugated eigenvalue pairs N_c . For every point (E, ω) the cardinality is given by $|M| = 3^{N_c}$. For the modified Markovianity test, we first set $N_b = 1$ (since in general this has given us the most efficient results) and varied η . The latter essentially sets a new number of ‘relevant’ complex conjugated eigenvalue pairs \tilde{N}_c which represents the number of modes which are insufficiently peaked. Note that $0 \leq \tilde{N}_c \leq N_c$. The cardinality $|M|$ for this method is given by $|M| = (N_b + 1)^{\tilde{N}_c} + 1$, where we add the $+1$ term for the generator of the principle branch \mathcal{S}_0 , which we always check first. The results for $|M|$ for the different methods and points are shown in Tab. I. For the modified Markovianity test, the cardinality is on average $|M| \approx 10^5$ over the considered ω -interval, which we plot in Fig. 2(a) of the main text for $L = 3$ (red).

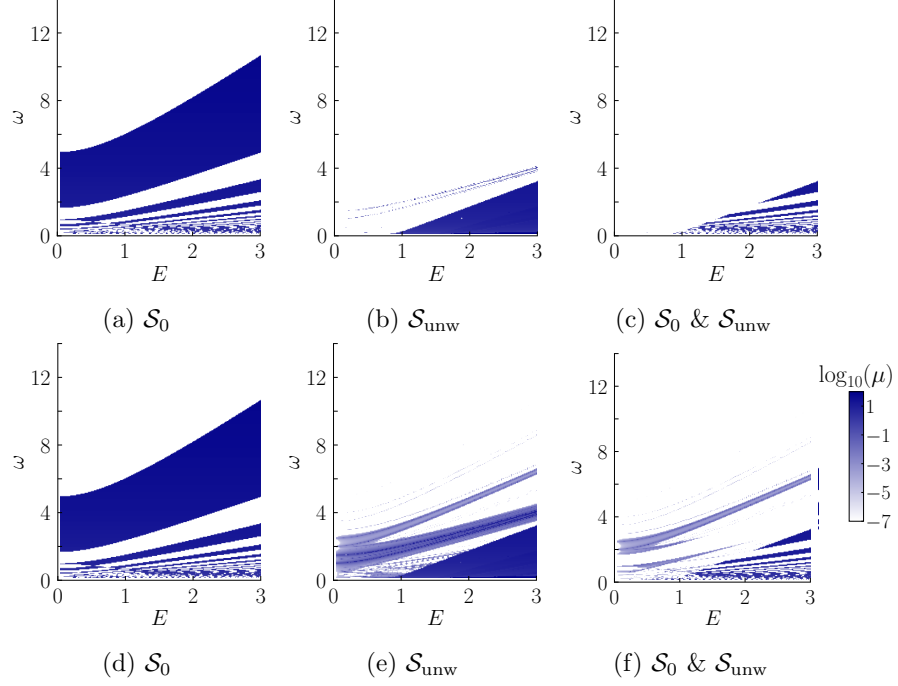


FIG. 3. (a)-(f) Distance from Markovianity μ of the effective generator of the one-cycle evolution superoperator as a function of driving strength E and frequency ω , for a coupling strength $w = 0.1$, a chain length of $L = 2$ and (a)-(c) $\gamma = 0$ and (d)-(f) $\gamma = 0.01$. To lift the degeneracy, we set the energy splittings to $\Delta_1 = 1.01$, $\Delta_2 = 1.00$, $\Delta_3 = 0.98$.

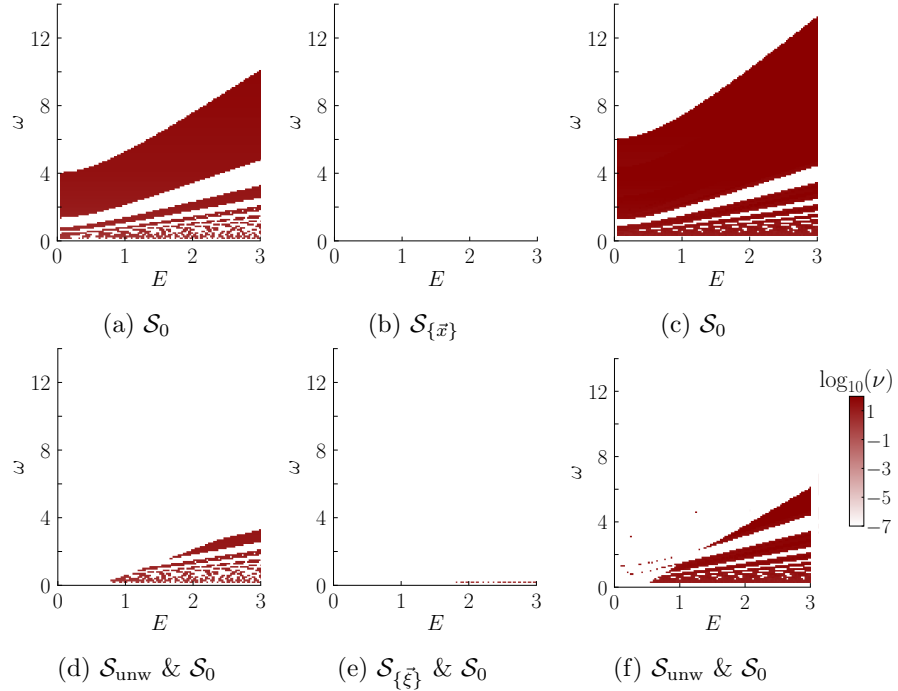


FIG. 4. (a)-(f) Distance from von Neumann form ν of the effective generator of the one-cycle evolution superoperator as a function of driving strength E and frequency ω , for no dissipation, $\gamma = 0$, coupling strength $w = 0.1$, and chain lengths of (a),(b),(d),(e) $L = 2$ and (c),(f) $L = 3$. We set $\Delta_1 = 1.01$, $\Delta_2 = 1.00$, $\Delta_3 = 0.98$.

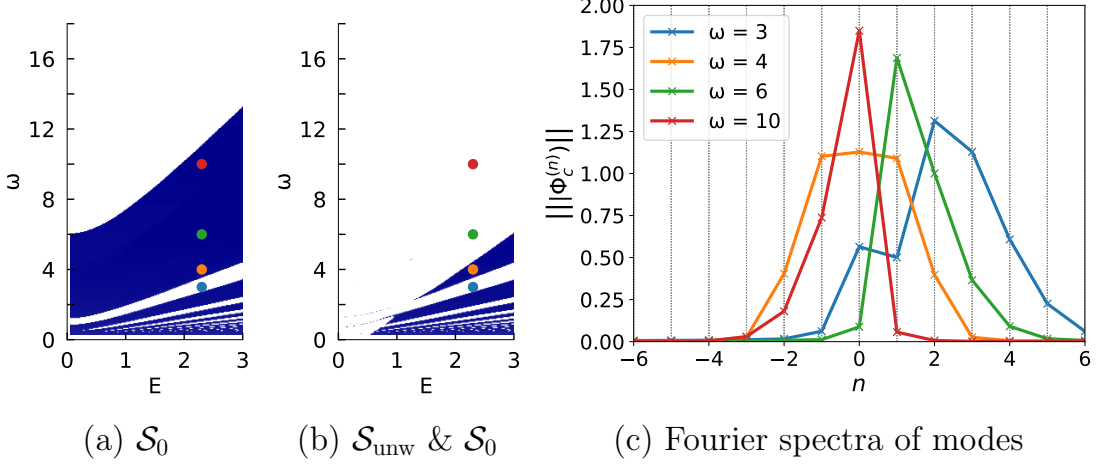


FIG. 5. (a) and (b) same as in Fig. 1(c) and (f) of the main text, respectively. (c) Fourier spectrum analysis of $\|\Phi_c^{(n)}\|$ for a specific Floquet mode c , as a function of n . The different curves correspond to the points in (a) and (b). We observe that for $\omega = 4$ (orange), where the procedure fails for \mathcal{S}_{unw} , $\|\Phi_c^{(-1)}\|$, $\|\Phi_c^{(0)}\|$, $\|\Phi_c^{(+1)}\|$ are very close to each other such that here, all three n should be considered. On the other hand, for the other frequencies ω , for which the procedure works well, the amplitudes are peaked distinctly.

	ω	3.8	3.9	4.0	4.1	4.2	4.3	4.4	4.5	4.6	4.7	4.8	4.9	5.0	...	11.7
mod. Markovianity test ($N_b = 1$)	η	0.72	0.69	0.68	0.68	0.69	0.93	0.94	0.95	0.96	0.97	0.98	0.99	-	...	-
	\tilde{N}_c	20	22	22	22	20	13	13	10	7	6	2	2	0	...	0
stan. Markovianity test ($x_c \in \{-1, 0, 1\}$)	N_c	28	28	28	28	28	28	28	28	28	28	28	28	28	...	28
	$ M $	3^{20}	3^{22}	3^{22}	3^{22}	3^{20}	2^{13}	2^{13}	2^{10}	2^7	2^6	2^2	2^2	2	...	3^{28}

TABLE I. Comparison of the complexity of the modified and the standard Markovianity test for a spin chain of length $L = 3$, driving strength of $E = 2.5$ and no dissipation ($\gamma = 0$). Note that for both methods we show the minimal cardinality $|M|$ which yields proper von Neumann generators for every point in the considered ω -Intervall.

Appendix E: Phase diagrams for interacting systems and other forms of dissipation

Consider the Hamiltonian of the main text, i.e. a circularly driven spin chain of length L ,

$$H(t) = \sum_{\ell=1}^L \frac{\Delta_\ell}{2} \sigma_z^\ell + \sum_{\ell=1}^{L-1} w \sigma_x^\ell \sigma_x^{\ell+1} + H_{\text{drive}}(t) \quad (\text{E1})$$

$$H_{\text{drive}}(t) = \sum_{\ell=1}^L E [\cos(\omega t) \sigma_x^\ell - \sin(\omega t) \sigma_y^\ell], \quad (\text{E2})$$

with level splittings Δ_ℓ and coupling strengths w between neighbouring spins. For a chain length of $L = 3$ we add dissipation from decay to every spin according to the total Lindbladian

$$\mathcal{L}(t)[\cdot] = -i[H(t), \cdot] + \sum_j \gamma (\sigma_-^j \cdot \sigma_+^j - \frac{1}{2} \{\sigma_+^j \sigma_-^j, \cdot\}), \quad (\text{E3})$$

where $\gamma = 0.01$. For interacting systems we generally observe that even for very small coupling strengths w ,

we see a non-Markovian background arising and growing with increasing w , as we can see in Fig. 7. Now recall that the most general form of a Lindbladian (i.e. a generator of a quantum dynamical semigroup $\mathcal{V}(t) = e^{\mathcal{L}t}$) is given by [55],[56]

$$\mathcal{L}[\cdot] = -i[H, \cdot] + \sum_{i,j=1}^{d^2-1} G_{ij} \left(F_i \cdot F_j^\dagger - \frac{1}{2} \{ F_j^\dagger F_i, \cdot \} \right), \quad (\text{E4})$$

where G_{ij} a positive semidefinite Kossakowski matrix, and F_i a basis of traceless operators. Note that for the model in Eq. (E3) the original Kossakowski matrix is very sparse, so that in the effective Lindbladian, many small but positive and negative eigenvalues of the effective Kossakowski matrix can be generated. We therefore observe that the emergence of non-Markovian areas for even weakly interacting systems can be counteracted by allowing dissipation from several dissipation channels, i.e. high-rank Kossakowski matrices G_{ij} . Motivated by this observation, to avoid large non-Markovian regimes at finite interaction w , we chose the particular type of

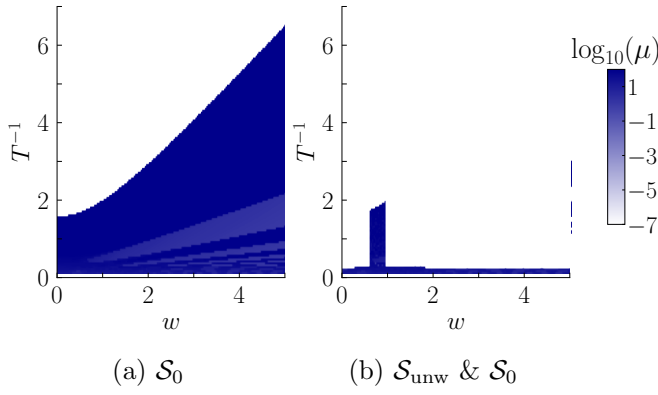


FIG. 6. Distance from Markovianity μ of the effective generator of the evolution superoperator $\mathcal{V}(T)$ as a function of coupling strength w and inverse observation time T^{-1} , for $\gamma = 0.01$, $\lambda = 0.5$ a chain length of $L = 3$. The energy splittings are set to $\Delta_1 = 2.45$, $\Delta_2 = 1.02$, $\Delta_3 = 1.65$.

dissipation in the main

$$\mathcal{L}(t)[\cdot] = -i[H(t), \cdot] + \sum_{\ell=1}^L \sum_{k,q} (L_{kq}^\ell \cdot L_{kq}^{\ell\dagger} - \frac{1}{2} \{L_{kq}^{\ell\dagger} L_{kq}^\ell, \cdot\}), \quad (E5)$$

where for the specific form of the Lindblad jump operators L_{kq} we refer to the main text.

Appendix F: non-Floquet problem

To investigate and demonstrate the spectral unwinding procedure for a system that does not stem from a Floquet

problem, we consider the Hamiltonian from the main text

$$H = \sum_{\ell=1}^L \frac{\Delta_\ell}{2} \sigma_z^\ell + \sum_{\ell=1}^{L-1} w \sigma_x^\ell \sigma_x^{\ell+1} \quad (F1)$$

but with $H_{\text{drive}}(t) = 0$. We now define two different Lindbladians

$$\mathcal{L}_1[\cdot] = -i[H, \cdot] + \sum_{\ell=1}^L \gamma (\sigma_x^\ell \cdot \sigma_x^\ell - \frac{1}{2} \{\sigma_x^\ell \sigma_x^\ell, \cdot\}) \quad (F2)$$

$$\mathcal{L}_2[\cdot] = -i[H, \cdot] + \sum_{\ell=1}^L \gamma (\sigma_y^\ell \cdot \sigma_y^\ell - \frac{1}{2} \{\sigma_y^\ell \sigma_y^\ell, \cdot\}). \quad (F3)$$

We formally solve the respective master equations generated by the individual Lindbladians,

$$\frac{\partial}{\partial t} \rho = \mathcal{L}_j[\rho], \quad (F4)$$

and extract the maps $\mathcal{V}_j(t) = e^{t\mathcal{L}_j}$. We now define the dynamical map (Ref. [63])

$$\mathcal{V}(t) = \lambda \mathcal{V}_1(t) + (1 - \lambda) \mathcal{V}_2(t), \quad (F5)$$

where $\lambda \in [0, 1]$. We investigate its dynamics up to a given observation time T . To extract the effective generators and test them for Markovianity, we take the logarithm of $\mathcal{V}(T)$ and apply the Markovianity test outlined in the main text. In Fig. 6 we can see that the unwinded generator \mathcal{S}_{unw} again produces valid effective Lindbladians in a large area where the generator of the principle branch \mathcal{S}_0 does not.

[1] E. Altman, K. R. Brown, G. Carleo, L. D. Carr, E. Demler, C. Chin, B. DeMarco, S. E. Economou, M. A. Eriksen, K.-M. C. Fu, M. Greiner, K. R. Hazzard, R. G. Hulet, A. J. Kollár, B. L. Lev, M. D. Lukin, R. Ma, X. Mi, S. Misra, C. Monroe, K. Murch, Z. Nazario, K.-K. Ni, A. C. Potter, P. Roushan, M. Saffman, M. Schleier-Smith, I. Siddiqi, R. Simmonds, M. Singh, I. Spielman, K. Temme, D. S. Weiss, J. Vučković, V. Vuletić, J. Ye, and M. Zwierlein, Quantum Simulators: Architectures and Opportunities, *PRX Quantum* **2**, 017003 (2021).

[2] J. Preskill, Quantum Computing in the NISQ era and beyond, *Quantum* **2**, 79 (2018).

[3] M. Aidelsburger, M. Atala, S. Nascimbène, S. Trotzky, Y.-A. Chen, and I. Bloch, Experimental Realization of Strong Effective Magnetic Fields in an Optical Lattice, *Phys. Rev. Lett.* **107**, 255301 (2011).

[4] M. Aidelsburger, M. Atala, M. Lohse, J. T. Barreiro, B. Paredes, and I. Bloch, Realization of the Hofstadter Hamiltonian with Ultracold Atoms in Optical Lattices, *Physical Review Letters* **111**, 185301 (2013).

[5] N. Goldman, J. Dalibard, M. Aidelsburger, and N. R. Cooper, Periodically-driven quantum matter: The case of resonant modulations, *Phys. Rev. A* **91**, 033632 (2015).

[6] A. Eckardt, Colloquium: Atomic quantum gases in periodically driven optical lattices, *Reviews of Modern Physics* **89**, 011004 (2017).

[7] L. W. Clark, N. Schine, C. Baum, N. Jia, and J. Simon, Observation of Laughlin states made of light, *Nature* **582**, 41 (2020).

[8] D. Jafferis, A. Zlokapa, J. D. Lykken, D. K. Kolchmeyer, S. I. Davis, N. Lauk, H. Neven, and M. Spiropulu, Traversable wormhole dynamics on a quantum processor, *Nature* **612**, 51 (2022).

[9] K. J. Satzinger, Y.-J. Liu, A. Smith, C. Knapp, M. Newman, C. Jones, Z. Chen, C. Quintana, X. Mi, A. Dunsworth, C. Gidney, I. Aleiner, F. Arute, K. Arya, J. Atalaya, R. Babbush, J. C. Bardin, R. Barends, J. Basso, A. Bengtsson, A. Bilmes, M. Broughton, B. B. Buckley, D. A. Buell, B. Burkett, N. Bushnell, B. Chiaro, R. Collins, W. Courtney, S. Demura, A. R. Derk, D. Eppens, C. Erickson, L. Faoro, E. Farhi, A. G. Fowler, B. Foxen, M. Giustina, A. Greene, J. A. Gross, M. P.

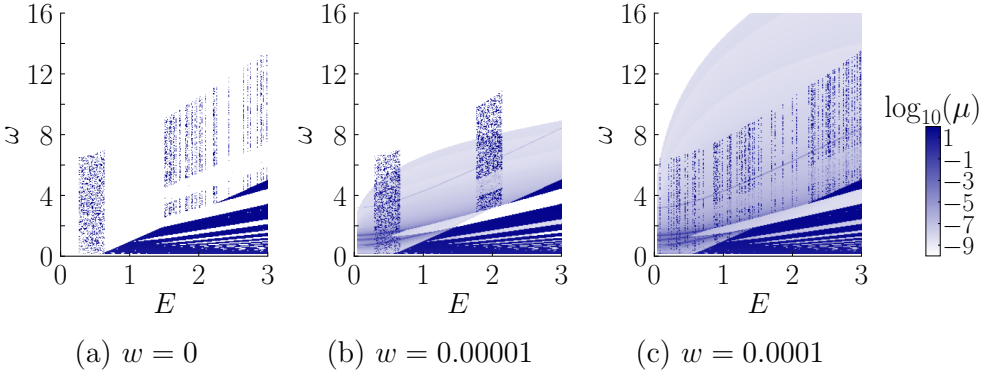


FIG. 7. Distance from Markovianity μ of the effective generator of the one-cycle evolution superoperator as a function of driving strength E and frequency ω , for coupling strengths (a) $w = 0$, (b) $w = 0.00001$, (c) $w = 0.0001$, a chain length of $L = 3$, with dissipation from decay and a dissipation parameter of $\gamma = 0.01$. Energy splittings are $\Delta_1 = 1.4$, $\Delta_2 = 1.1$, $\Delta_3 = 0.7$. For all plots we consider \mathcal{S}_0 and \mathcal{S}_{unw} .

Harrigan, S. D. Harrington, J. Hilton, S. Hong, T. Huang, W. J. Huggins, L. B. Ioffe, S. V. Isakov, E. Jeffrey, Z. Jiang, D. Kafri, K. Kechedzhi, T. Khattar, S. Kim, P. V. Klimov, A. N. Korotkov, F. Kostritsa, D. Landhuis, P. Laptev, A. Locharla, E. Lucero, O. Martin, J. R. McClean, M. McEwen, K. C. Miao, M. Mohseni, S. Montazeri, W. Mruczkiewicz, J. Mutus, O. Naaman, M. Neeley, C. Neill, M. Y. Niu, T. E. O'Brien, A. Opremcak, B. Pató, A. Petukhov, N. C. Rubin, D. Sank, V. Shvarts, D. Strain, M. Szalay, B. Villalonga, T. C. White, Z. Yao, P. Yeh, J. Yoo, A. Zalcman, H. Neven, S. Boixo, A. Megrant, Y. Chen, J. Kelly, V. Smelyanskiy, A. Kitaev, M. Knap, F. Pollmann, and P. Roushan, Realizing topologically ordered states on a quantum processor, *Science* **374**, 1237 (2021).

[10] R. N. Tazhigulov, S.-N. Sun, R. Haghshenas, H. Zhai, A. T. Tan, N. C. Rubin, R. Babbush, A. J. Minnich, and G. K.-L. Chan, Simulating Models of Challenging Correlated Molecules and Materials on the Sycamore Quantum Processor, *PRX Quantum* **3**, 040318 (2022).

[11] J. Léonard, S. Kim, J. Kwan, P. Segura, F. Grusdt, C. Repellin, N. Goldman, and M. Greiner, Realization of a fractional quantum Hall state with ultracold atoms, *Nature* **619**, 495 (2023).

[12] J. Kwan, P. Segura, Y. Li, S. Kim, A. V. Gorshkov, A. Eckardt, B. Bakkali-Hassani, and M. Greiner, Realization of 1D Anyons with Arbitrary Statistical Phase (2023), arXiv:2306.01737 [cond-mat, physics:physics, physics:quant-ph].

[13] T. I. Andersen, Y. D. Lensky, K. Kechedzhi, I. K. Drozdov, A. Bengtsson, S. Hong, A. Morvan, X. Mi, A. Opremcak, R. Acharya, R. Allen, M. Ansmann, F. Arute, K. Arya, A. Asfaw, J. Atalaya, R. Babbush, D. Bacon, J. C. Bardin, G. Bortoli, A. Bourassa, J. Bovaard, L. Brill, M. Broughton, B. B. Buckley, D. A. Buell, T. Burger, B. Burkett, N. Bushnell, Z. Chen, B. Chiaro, D. Chik, C. Chou, J. Cogan, R. Collins, P. Conner, W. Courtney, A. L. Crook, B. Curtin, D. M. Debroy, A. Del Toro Barba, S. Demura, A. Dunsworth, D. Eppens, C. Erickson, L. Faoro, E. Farhi, R. Fatemi, L. Flores Burgos, E. Forati, A. G. Fowler, B. Foxen, W. Giang, C. Gidney, D. Gilboa, M. Giustina, A. Grajales Dau, J. A. Gross, S. Habegger, M. C. Hamilton, M. P. Harrigan, S. D. Harrington, O. Higgott, J. Hilton, M. Hoffmann, S. Hong, T. Huang, A. Huff, W. J. Huggins, L. B. Ioffe, S. V. Isakov, J. Iveland, E. Jeffrey, Z. Jiang, C. Jones, P. Juhas, M. Hansen, M. P. Harrigan, S. D. Harrington, P. Heu, J. Hilton, M. R. Hoffmann, T. Huang, A. Huff, W. J. Huggins, L. B. Ioffe, S. V. Isakov, J. Iveland, E. Jeffrey, Z. Jiang, C. Jones, P. Juhas, D. Kafri, T. Khattar, M. Khezri, M. Kieferová, S. Kim, A. Kitaev, P. V. Klimov, A. R. Klots, A. N. Korotkov, F. Kostritsa, J. M. Kreikebaum, D. Landhuis, P. Laptev, K.-M. Lau, L. Laws, J. Lee, K. W. Lee, B. J. Lester, A. T. Lill, W. Liu, A. Locharla, E. Lucero, F. D. Malone, O. Martin, J. R. McClean, T. McCourt, M. McEwen, K. C. Miao, A. Mieszala, M. Mohseni, S. Montazeri, E. Mount, R. Movassagh, W. Mruczkiewicz, O. Naaman, M. Neeley, C. Neill, A. Nersisyan, M. Newman, J. H. Ng, A. Nguyen, M. Nguyen, M. Y. Niu, T. E. O'Brien, S. Omonije, A. Petukhov, R. Potter, L. P. Pryadko, C. Quintana, C. Rocque, N. C. Rubin, N. Saei, D. Sank, K. Sankaragomathi, K. J. Satzinger, H. F. Schurkus, C. Schuster, M. J. Shearn, A. Shorter, N. Shutty, V. Shvarts, J. Skrzyni, W. C. Smith, R. Somma, G. Sterling, D. Strain, M. Szalay, A. Torres, G. Vidal, B. Villalonga, C. V. Heidweiller, T. White, B. W. K. Woo, C. Xing, Z. J. Yao, P. Yeh, J. Yoo, G. Young, A. Zalcman, Y. Zhang, N. Zhu, N. Zobrist, H. Neven, S. Boixo, A. Megrant, J. Kelly, Y. Chen, V. Smelyanskiy, E.-A. Kim, I. Aleiner, P. Roushan, and Google Quantum AI and Collaborators, Non-Abelian braiding of graph vertices in a superconducting processor, *Nature* **618**, 264 (2023).

[14] R. Acharya, I. Aleiner, R. Allen, T. I. Andersen, M. Ansmann, F. Arute, K. Arya, A. Asfaw, J. Atalaya, R. Babbush, D. Bacon, J. C. Bardin, J. Basso, A. Bengtsson, S. Boixo, G. Bortoli, A. Bourassa, J. Bovaard, L. Brill, M. Broughton, B. B. Buckley, D. A. Buell, T. Burger, B. Burkett, N. Bushnell, Y. Chen, Z. Chen, B. Chiaro, J. Cogan, R. Collins, P. Conner, W. Courtney, A. L. Crook, B. Curtin, D. M. Debroy, A. Del Toro Barba, S. Demura, A. Dunsworth, D. Eppens, C. Erickson, L. Faoro, E. Farhi, R. Fatemi, L. Flores Burgos, E. Forati, A. G. Fowler, B. Foxen, W. Giang, C. Gidney, D. Gilboa, M. Giustina, A. Grajales Dau, J. A. Gross, S. Habegger, M. C. Hamilton, M. P. Harrigan, S. D. Harrington, O. Higgott, J. Hilton, M. Hoffmann, S. Hong, T. Huang, A. Huff, W. J. Huggins, L. B. Ioffe, S. V. Isakov, J. Iveland, E. Jeffrey, Z. Jiang, C. Jones, P. Juhas,

D. Kafri, K. Kechedzhi, J. Kelly, T. Khattar, M. Khezri, M. Kieferová, S. Kim, A. Kitaev, P. V. Klimov, A. R. Klots, A. N. Korotkov, F. Kostritsa, J. M. Kreikebaum, D. Landhuis, P. Laptev, K.-M. Lau, L. Laws, J. Lee, K. Lee, B. J. Lester, A. Lill, W. Liu, A. Locharla, E. Lucero, F. D. Malone, J. Marshall, O. Martin, J. R. McClean, T. McCourt, M. McEwen, A. Megrant, B. Meurer Costa, X. Mi, K. C. Miao, M. Mohseni, S. Montazeri, A. Morvan, E. Mount, W. Mruczkiewicz, O. Naaman, M. Neeley, C. Neill, A. Nersisyan, H. Neven, M. Newman, J. H. Ng, A. Nguyen, M. Nguyen, M. Y. Niu, T. E. O'Brien, A. Opremcak, J. Platt, A. Petukhov, R. Potter, L. P. Pryadko, C. Quintana, P. Roushan, N. C. Rubin, N. Saei, D. Sank, K. Sankaragomathi, K. J. Satzinger, H. F. Schurkus, C. Schuster, M. J. Shearn, A. Shorter, V. Shvarts, J. Skrzyni, V. Smelyanskiy, W. C. Smith, G. Sterling, D. Strain, M. Szalay, A. Torres, G. Vidal, B. Villalonga, C. Vollgraff Heidweiller, T. White, C. Xing, Z. J. Yao, P. Yeh, J. Yoo, G. Young, A. Zalcman, Y. Zhang, N. Zhu, and Google Quantum AI, Suppressing quantum errors by scaling a surface code logical qubit, *Nature* **614**, 676 (2023).

[15] D. Bluvstein, S. J. Evered, A. A. Geim, S. H. Li, H. Zhou, T. Manovitz, S. Ebadi, M. Cain, M. Kalinowski, D. Hangleiter, J. P. Bonilla Ataides, N. Maskara, I. Cong, X. Gao, P. Sales Rodriguez, T. Karolyshyn, G. Semeghini, M. J. Gullans, M. Greiner, V. Vuletić, and M. D. Lukin, Logical quantum processor based on reconfigurable atom arrays, *Nature* **626**, 58 (2024).

[16] R. Acharya, L. Aghababaie-Beni, I. Aleiner, T. I. Andersen, M. Ansmann, F. Arute, K. Arya, A. Asfaw, N. Asstrakhantsev, J. Atalaya, R. Babbush, D. Bacon, B. Ballard, J. C. Bardin, J. Bausch, A. Bengtsson, A. Bilmes, S. Blackwell, S. Boixo, G. Bortoli, A. Bourassa, J. Boavaard, L. Brill, M. Broughton, D. A. Browne, B. Buchea, B. B. Buckley, D. A. Buell, T. Burger, B. Burkett, N. Bushnell, A. Cabrera, J. Campero, H.-S. Chang, Y. Chen, Z. Chen, B. Chiaro, D. Chik, C. Chou, J. Claes, A. Y. Cleland, J. Cogan, R. Collins, P. Conner, W. Courtney, A. L. Crook, B. Curtin, S. Das, A. Davies, L. De Lorenzo, D. M. Debroy, S. Demura, M. Devoret, A. Di Paolo, P. Donohoe, I. Drozdov, A. Dunsworth, C. Earle, T. Edlich, A. Eickbusch, A. M. Elbag, M. Elzouka, C. Erickson, L. Faoro, E. Farhi, V. S. Ferreira, L. F. Burgos, E. Forati, A. G. Fowler, B. Foxen, S. Gajjam, G. Garcia, R. Gasca, É. Genois, W. Giang, C. Gidney, D. Gilboa, R. Gosula, A. G. Dau, D. Graumann, A. Greene, J. A. Gross, S. Habegger, J. Hall, M. C. Hamilton, M. Hansen, M. P. Harrigan, S. D. Harrington, F. J. H. Heras, S. Heslin, P. Heu, O. Higgott, G. Hill, J. Hilton, G. Holland, S. Hong, H.-Y. Huang, A. Huff, W. J. Huggins, L. B. Ioffe, S. V. Isakov, J. Iveland, E. Jeffrey, Z. Jiang, C. Jones, S. Jordan, C. Joshi, P. Juhas, D. Kafri, H. Kang, A. H. Karamlou, K. Kechedzhi, J. Kelly, T. Khaire, T. Khattar, M. Khezri, S. Kim, P. V. Klimov, A. R. Klots, B. Koprin, P. Kohli, A. N. Korotkov, F. Kostritsa, R. Kothari, B. Kozlovskii, J. M. Kreikebaum, V. D. Kurilovich, N. Lacroix, D. Landhuis, T. Lange-Dei, B. W. Langley, P. Laptev, K.-M. Lau, L. L. Guevel, J. Ledford, K. Lee, Y. D. Lensky, S. Leon, B. J. Lester, W. Y. Li, Y. Li, A. T. Lill, W. Liu, W. P. Livingston, A. Locharla, E. Lucero, D. Lundahl, A. Lunt, S. Madhuk, F. D. Malone, A. Maloney, S. Mandrá, L. S. Martin, S. Martin, O. Martin, C. Maxfield, J. R. McClean, M. McEwen, S. Meeks, A. Megrant, X. Mi, K. C. Miao, A. Mieszala, R. Molavi, S. Molina, S. Montazeri, A. Morvan, R. Movassagh, W. Mruczkiewicz, O. Naaman, M. Neeley, C. Neill, A. Nersisyan, H. Neven, M. Newman, J. H. Ng, A. Nguyen, M. Nguyen, C.-H. Ni, T. E. O'Brien, W. D. Oliver, A. Opremcak, K. Ottosson, A. Petukhov, A. Pizzuto, J. Platt, R. Potter, O. Pritchard, L. P. Pryadko, C. Quintana, G. Ramachandran, M. J. Reagor, D. M. Rhodes, G. Roberts, E. Rosenberg, E. Rosenfeld, P. Roushan, N. C. Rubin, N. Saei, D. Sank, K. Sankaragomathi, K. J. Satzinger, H. F. Schurkus, C. Schuster, A. W. Senior, M. J. Shearn, A. Shorter, N. Shutty, V. Shvarts, S. Singh, V. Sivak, J. Skrzyni, S. Small, V. Smelyanskiy, W. C. Smith, R. D. Somma, S. Springer, G. Sterling, D. Strain, J. Suchard, A. Szasz, A. Sztein, D. Thor, A. Torres, M. M. Torunbalci, A. Vaishnav, J. Vargas, S. Vdovichev, G. Vidal, B. Villalonga, C. V. Heidweiller, S. Waltman, S. X. Wang, B. Ware, K. Weber, T. White, K. Wong, B. W. K. Woo, C. Xing, Z. J. Yao, P. Yeh, B. Ying, J. Yoo, N. Yosri, G. Young, A. Zalcman, Y. Zhang, N. Zhu, and N. Zobrist, Quantum error correction below the surface code threshold (2024), arXiv:2408.13687 [quant-ph].

[17] S. Xu, Z.-Z. Sun, K. Wang, H. Li, Z. Zhu, H. Dong, J. Deng, X. Zhang, J. Chen, Y. Wu, C. Zhang, F. Jin, X. Zhu, Y. Gao, A. Zhang, N. Wang, Y. Zou, Z. Tan, F. Shen, J. Zhong, Z. Bao, W. Li, W. Jiang, L.-W. Yu, Z. Song, P. Zhang, L. Xiang, Q. Guo, Z. Wang, C. Song, H. Wang, and D.-L. Deng, Non-Abelian braiding of Fibonacci anyons with a superconducting processor, *Nature Physics* **20**, 1469 (2024).

[18] C. Wang, F.-M. Liu, M.-C. Chen, H. Chen, X.-H. Zhao, C. Ying, Z.-X. Shang, J.-W. Wang, Y.-H. Huo, C.-Z. Peng, X. Zhu, C.-Y. Lu, and J.-W. Pan, Realization of fractional quantum Hall state with interacting photons, *Science* **384**, 579 (2024).

[19] M. Lukin, L. D'Alessio, and A. Polkovnikov, Universal High-Frequency Behavior of Periodically Driven Systems: From Dynamical Stabilization to Floquet Engineering, *Adv. in Phys.* **64**, 139 (2015).

[20] A. Eckardt and E. Anisimovas, High-frequency approximation for periodically driven quantum systems from a Floquet-space perspective, *New Journal of Physics* **17**, 093039 (2015).

[21] H. Zhao, F. Mintert, R. Moessner, and J. Knolle, Random Multipolar Driving: Tunably Slow Heating through Spectral Engineering, *Physical Review Letters* **126**, 040601 (2021).

[22] M. Suzuki, Relationship between d-Dimensional Quantum Spin Systems and (d+1)-Dimensional Ising Systems: Equivalence, Critical Exponents and Systematic Approximants of the Partition Function and Spin Correlations, *Progress of Theoretical Physics* **56**, 1454 (1976).

[23] W. Chen, M. Abbasi, B. Ha, S. Erdamar, Y. N. Joglekar, and K. W. Murch, Decoherence-Induced Exceptional Points in a Dissipative Superconducting Qubit, *Physical Review Letters* **128**, 110402 (2022).

[24] N. Wiebe, D. Berry, P. Høyer, and B. C. Sanders, Higher order decompositions of ordered operator exponentials, *Journal of Physics A: Mathematical and Theoretical* **43**, 065203 (2010).

[25] L. M. Sieberer, T. Olsacher, A. Elben, M. Heyl, P. Hauke, F. Haake, and P. Zoller, Digital quantum simulation, Trotter errors, and quantum chaos of the kicked top, *npj*

Quantum Information **5**, 1 (2019).

[26] A. M. Childs, Y. Su, M. C. Tran, N. Wiebe, and S. Zhu, Theory of Trotter Error with Commutator Scaling, Physical Review X **11**, 011020 (2021).

[27] L. Pastori, T. Olsacher, C. Kokail, and P. Zoller, Characterization and Verification of Trotterized Digital Quantum Simulation Via Hamiltonian and Liouvillian Learning, PRX Quantum **3**, 030324 (2022).

[28] H. Zhao, A. Chen, S.-W. Liu, M. Bukov, M. Heyl, and R. Moessner, Learning effective Hamiltonians for adaptive time-evolution quantum algorithms (2024), arXiv:2406.06198 [cond-mat, physics:quant-ph].

[29] H. Zhao, M. Bukov, M. Heyl, and R. Moessner, Adaptive Trotterization for time-dependent Hamiltonian quantum dynamics using piecewise conservation laws, Physical Review Letters **133**, 010603 (2024), arXiv:2307.10327 [cond-mat, physics:quant-ph].

[30] M. Bukov and A. Polkovnikov, Stroboscopic versus non-stroboscopic dynamics in the Floquet realization of the Harper-Hofstadter Hamiltonian, Physical Review A **90**, 043613 (2014).

[31] N. Fläschner, B. S. Rem, M. Tarnowski, D. Vogel, D.-S. Lühmann, K. Sengstock, and C. Weitenberg, Experimental reconstruction of the Berry curvature in a Floquet Bloch band, Science **352**, 1091 (2016).

[32] M. Aidelsburger, Artificial gauge fields and topology with ultracold atoms in optical lattices, Journal of Physics B: Atomic, Molecular and Optical Physics **51**, 193001 (2018).

[33] K. Wintersperger, C. Braun, F. N. Ünal, A. Eckardt, M. D. Liberto, N. Goldman, I. Bloch, and M. Aidelsburger, Realization of an anomalous Floquet topological system with ultracold atoms, Nature Physics **16**, 1058 (2020).

[34] F. Petziol, M. Sameti, S. Carretta, S. Wimberger, and F. Mintert, Quantum Simulation of Three-Body Interactions in Weakly Driven Quantum Systems, Physical Review Letters **126**, 250504 (2021).

[35] F. Petziol, Non-Abelian Anyons in Periodically Driven Abelian Spin Liquids, Physical Review Letters **133**, 036601 (2024).

[36] B.-Y. Sun, N. Goldman, M. Aidelsburger, and M. Bukov, Engineering and Probing Non-Abelian Chiral Spin Liquids Using Periodically Driven Ultracold Atoms, PRX Quantum **4**, 020329 (2023).

[37] N. Goldman, O. Diessel, L. Barbiero, M. Prüfer, M. Di Liberto, and L. Peralta Gavensky, Floquet-Engineered Nonlinearities and Controllable Pair-Hopping Processes: From Optical Kerr Cavities to Correlated Quantum Matter, PRX Quantum **4**, 040327 (2023).

[38] F. Petziol, S. Wimberger, A. Eckardt, and F. Mintert, Nonperturbative Floquet engineering of the toric-code Hamiltonian and its ground state, Physical Review B **109**, 075126 (2024).

[39] D. Poilblanc, M. Mambrini, and N. Goldman, Floquet dynamical chiral spin liquid at finite frequency (2024), arXiv:2409.04892 [cond-mat, physics:quant-ph].

[40] F. Haddadfarshi, J. Cui, and F. Mintert, Completely Positive Approximate Solutions of Driven Open Quantum Systems, Phys. Rev. Lett. **114**, 130402 (2015).

[41] A. Schnell, A. Eckardt, and S. Denisov, Is there a Floquet Lindbladian?, Physical Review B **101**, 100301 (2020).

[42] A. Schnell, S. Denisov, and A. Eckardt, High-frequency expansions for time-periodic Lindblad generators, Physical Review B **104**, 165414 (2021).

[43] T. Mori, Floquet States in Open Quantum Systems, Annual Review of Condensed Matter Physics **14**, 35 (2023).

[44] K. Mizuta, *Nonequilibrium Quantum Many-Body Phenomena in Floquet Systems*, Doctoral thesis, Kyoto University (2022).

[45] Y.-A. Chen, A. M. Childs, M. Hafezi, Z. Jiang, H. Kim, and Y. Xu, Efficient product formulas for commutators and applications to quantum simulation, Physical Review Research **4**, 013191 (2022).

[46] D. Kolisnyk, F. Queißer, G. Schaller, and R. Schützhold, Floquet analysis of a superradiant many-qutrit refrigerator, Physical Review Applied **21**, 044050 (2024).

[47] S. Khandelwal, W. Chen, K. W. Murch, and G. Haack, Chiral Bell-State Transfer via Dissipative Liouvillian Dynamics, Physical Review Letters **133**, 070403 (2024).

[48] M. Hartmann, D. Poletti, M. Ivanchenko, S. Denisov, and P. Hänggi, Asymptotic Floquet states of open quantum systems: The role of interaction, New Journal of Physics **19**, 083011 (2017).

[49] C. M. Dai, H. Li, W. Wang, and X. X. Yi, Generalized Floquet theory for open quantum systems (2017), arXiv:1707.05030 [quant-ph].

[50] K. Mizuta, K. Takasan, and N. Kawakami, Breakdown of Markovianity by interactions in stroboscopic Floquet-Lindblad dynamics under high-frequency drive, Physical Review A **103**, L020202 (2021).

[51] T. Ikeda, K. Chinzei, and M. Sato, Nonequilibrium steady states in the Floquet-Lindblad systems: Van Vleck's high-frequency expansion approach, SciPost Physics Core **4**, 033 (2021).

[52] G. Cemin, M. Cech, E. Weiss, S. Soltan, D. Braun, I. Lesanovsky, and F. Carollo, Machine learning of quantum channels on NISQ devices (2024), arXiv:2405.12598 [cond-mat, physics:quant-ph].

[53] T. S. Cubitt, J. Eisert, and M. M. Wolf, The Complexity of Relating Quantum Channels to Master Equations, Communications in Mathematical Physics **310**, 383 (2012).

[54] M. M. Wolf, J. Eisert, T. S. Cubitt, and J. I. Cirac, Assessing non-markovian quantum dynamics, Physical Review Letters **101**, 150402 (2008).

[55] G. Lindblad, On the generators of quantum dynamical semigroups, Communications in Mathematical Physics **48**, 119 (1976).

[56] V. Gorini, A. Kossakowski, and E. C. G. Sudarshan, Completely positive dynamical semigroups of N-level systems, Journal of Mathematical Physics **17**, 821 (2008), https://pubs.aip.org/aip/jmp/article-pdf/17/5/821/8148306/821__1__online.pdf.

[57] To fulfil condition (i), negative real eigenvalues $\lambda_r < 0$ can only occur with an even degeneracy, such that one can reinterpret them as complex conjugated pairs.

[58] V. Volokitin, I. Meyerov, and S. Denisov, Machine learning approach to the Floquet-Lindbladian problem, Chaos: An Interdisciplinary Journal of Nonlinear Science **32**, 043117 (2022).

[59] F. N. Ünal, B. Seradjeh, and A. Eckardt, How to directly measure floquet topological invariants in optical lattices, Phys. Rev. Lett. **122**, 253601 (2019).

[60] H. Chen, Y.-M. Hu, W. Zhang, M. A. Kurniawan, Y. Shao, X. Chen, A. Prem, and X. Dai, Periodically

Driven Open Quantum Systems: Spectral Properties and Non-Equilibrium Steady States (2024), arXiv:2401.00131 [cond-mat, physics:quant-ph].

[61] M. Leskes, P. Madhu, and S. Vega, Floquet theory in solid-state nuclear magnetic resonance, *Progress in Nuclear Magnetic Resonance Spectroscopy* **57**, 345 (2010).

[62] H.-P. Breuer and F. Petruccione, *The Theory of Open Quantum Systems* (OUP Oxford, 2002).

[63] D. Chruściński, A. Kossakowski, and S. Pascazio, Long-time memory in non-Markovian evolutions, *Physical Review A* **81**, 10.1103/physreva.81.032101 (2010).